A controllable and dynamic assembly system based on discrete metallocages

Qihui Chen, Feilong Jiang, Daqiang Yuan, Guangxun Lyu, Lian Chen, Maochun Hong*

State Key Laboratory of Structure Chemistry, Fujian Institute of Research on the Structure of Matter, Chinese Academy of Sciences, Fuzhou, Fujian, P. R. China, 350002.

Experimental methods

General: All of reagents were commercially available and used as purchased. C, H, and N microanalyses were measured using an elemental Vairo EL analyzer, ^{1}HNMR and ^{19}FNMR and ^{13}CNMR spectra were recorded at Bruker AM-400 (400 MHZ) spectrometer, solid ^{19}FNMR and ^{13}CNMR were recorded at Bruker AVANCE III (500 MHZ) IR spectra were recorded on a Shimadzu IR-440 spectrometer.

Synthesis of compound 1

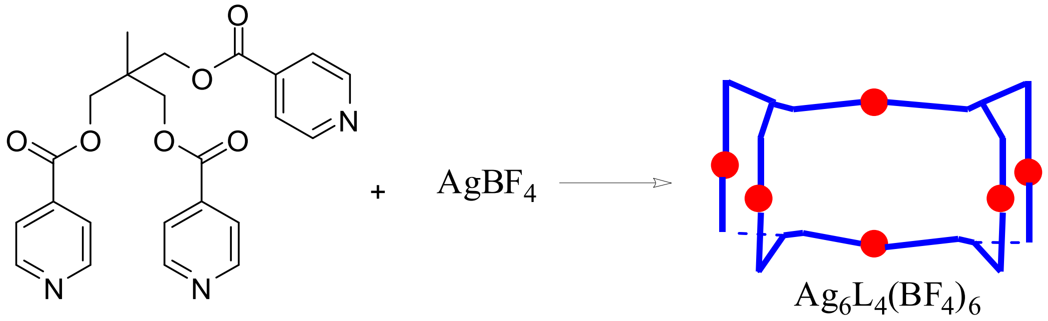

Scheme 1. *In situ* assembly of Ag_6L_4 cage.

Sonicating of 1mL MeOH solution of (5mg, 0.026mmol) $AgBF_4$ and 1mL $CHCl_3$ solution of (7mg, 0.016mmol) ligand **L** in 5 minutes gives a white powder

(10mg, yield: 86%), compound **1**. Anal. Calcd for [$Ag_6L_4(BF_4)_6$.0.85$CHCl_3$.2.2CH_3OH](%): C, 37.04; H, 3.06; N, 5.45; Found (%): C, 36.66; H, 3.50; N, 5.89. ^{1}HNMR (400 MHz, DMSO): δ: 8.80 (6H, d, *J*= 6), 7.94 (6H, d, *J*= 6), 4.55 (6H, s), 1.32 (3H, 3). ^{13}CNMR(400 MHz, DMSO): δ: 164.67, 151.75, 137.58, 123.54, 39.38, 17.28. ^{19}FNMR (400 MHz, DMSO): (-148). ESI-MS (m/z): 2820 [$Ag_6L_4(BF_4)_5$]$^+$. Solid ^{19}FNMR δ: -151. IR (KBr) *v* : 3620, 3109, 2978, 1734, 1616, 1560, 1425, 1332, 1283, 1129, 1063, 855, 759, 701, 521.

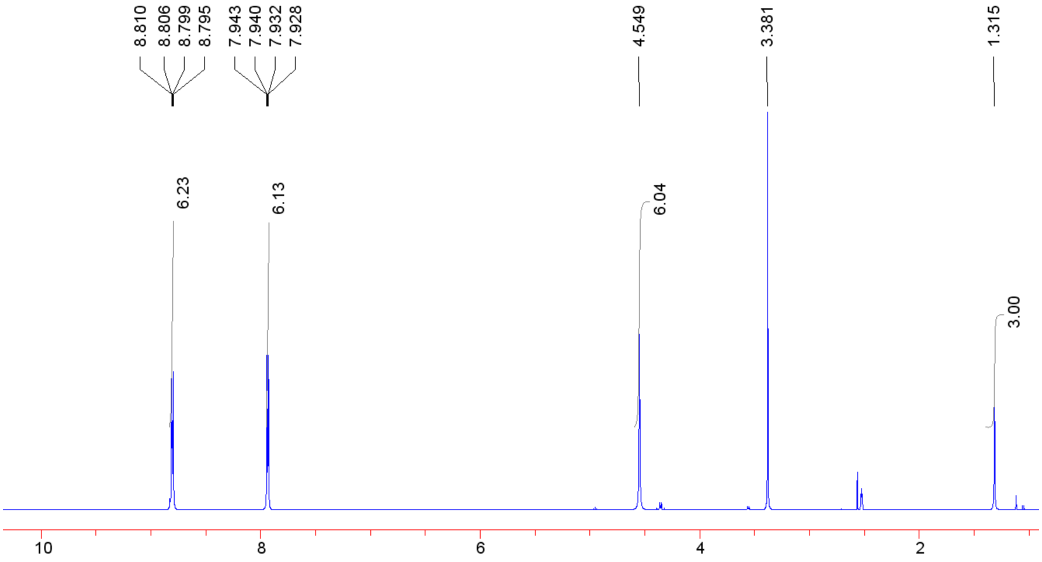

Figure 1. ^{1}HNMR (400 MHz, DMSO) of compound **1**.

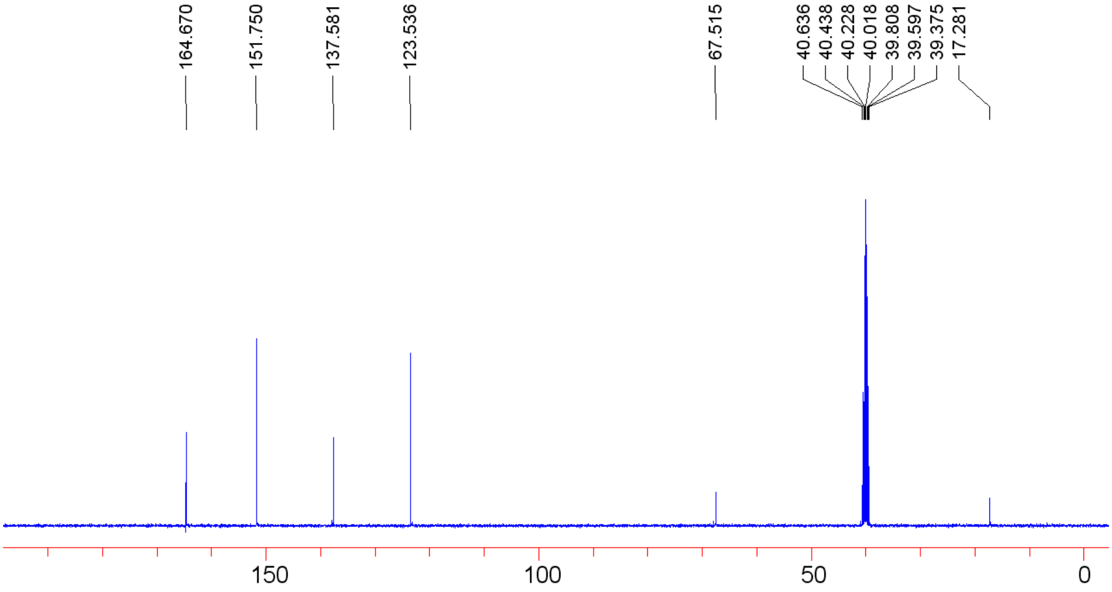

Figure 2. ^{13}CNMR (400 MHz, DMSO) of compound **1**.

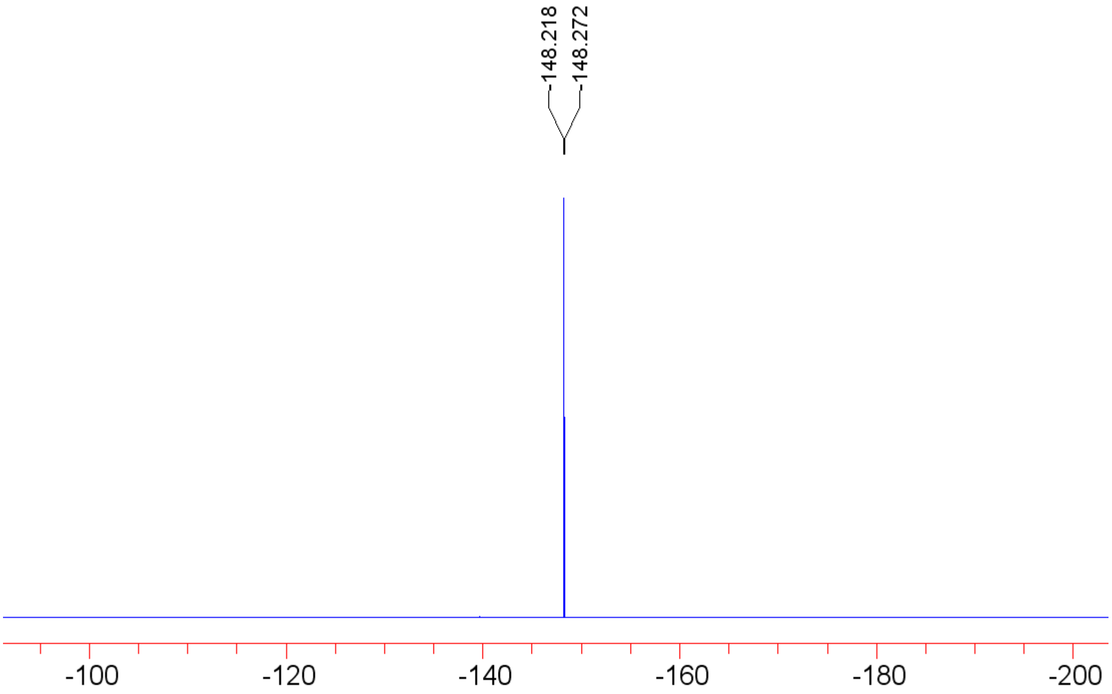

Figure 3. ^{19}FNMR (400 MHz, DMSO) of compound **1**.

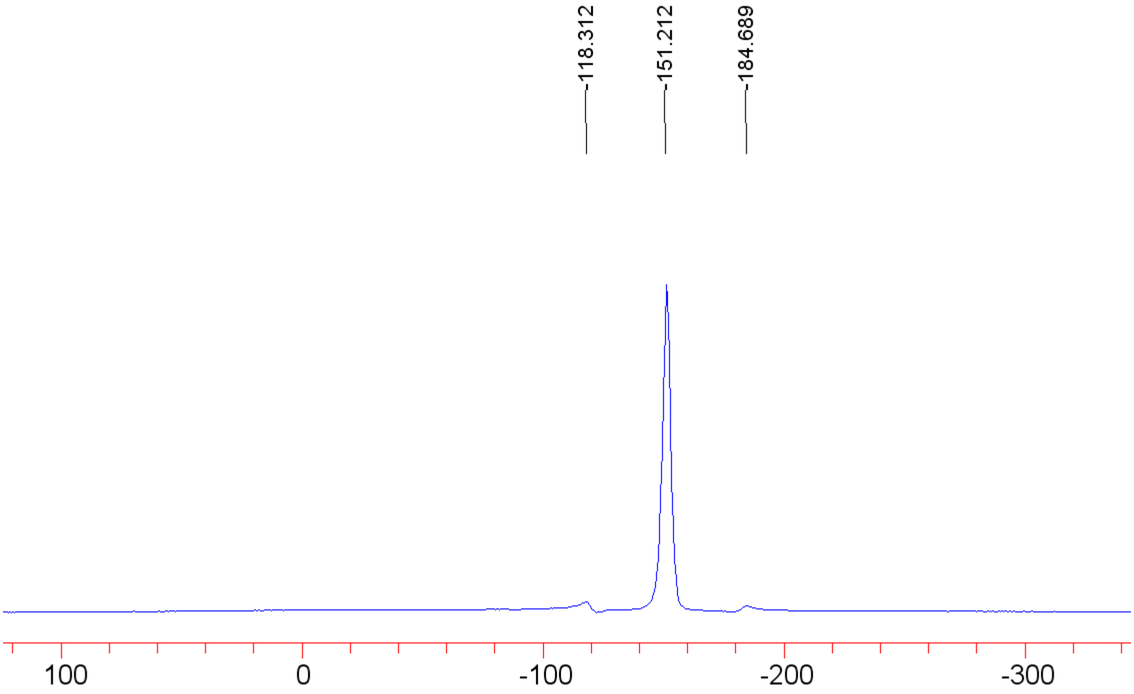

Figure 4. Solid ^{19}FNMR(500M) of compound **1**, in which the signals (-118 and -184) responds to the spinning sidebands of signal of -151.

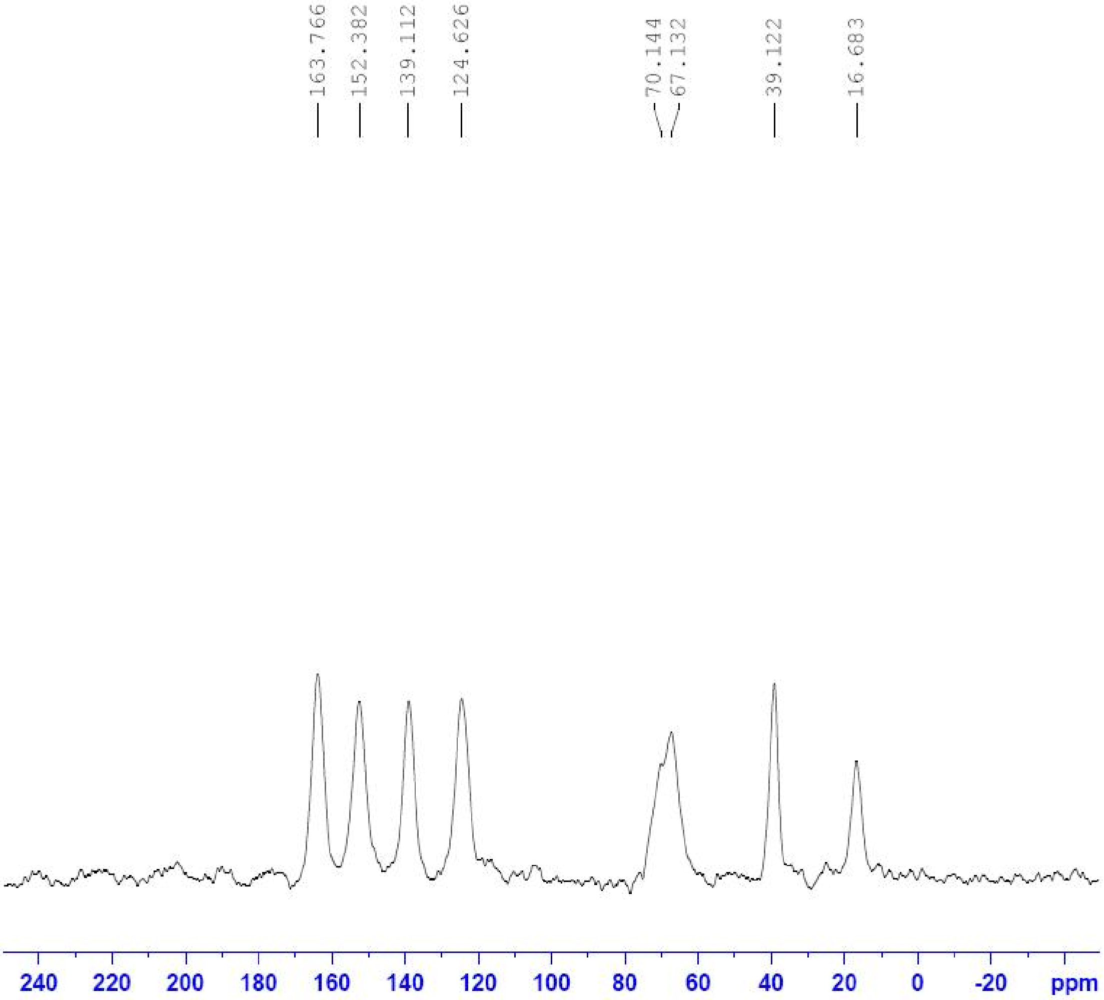

Figure 5. Solid ^{13}CNMR(500M) of compound **1**, the ligand L has only one type signal, which demonstrates that all of ligand L in compound **1** have same chemical atmosphere. So the compound **1** should not be Ag_5L_4, because ligand L comprised in Ag_5L_4 units should have different chemical atmosphere.

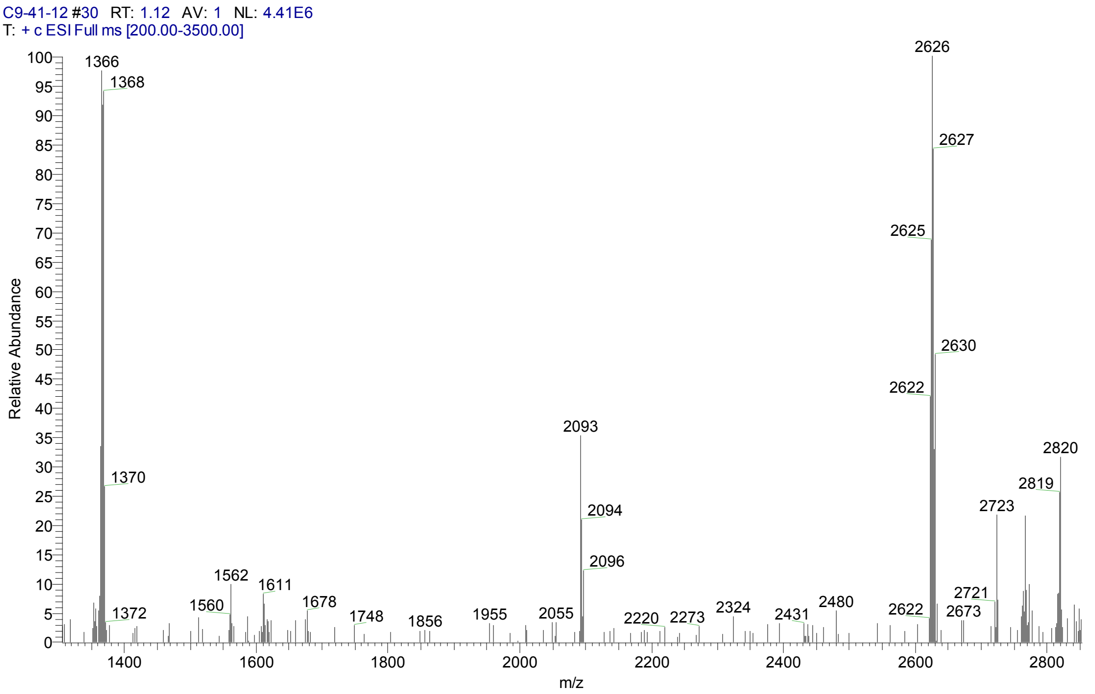

Figure 6. ESI-MS of compound **1** (DMSO solution), in which the peak 2820 responds to $[Ag_6L_4(BF_4)_5]^+$, the peak 1366 responds to $[Ag_6L_4(BF_4)_4]^{2+}$, the peak 2626 responds to $[Ag_5L_4(BF_4)_4]^+$.

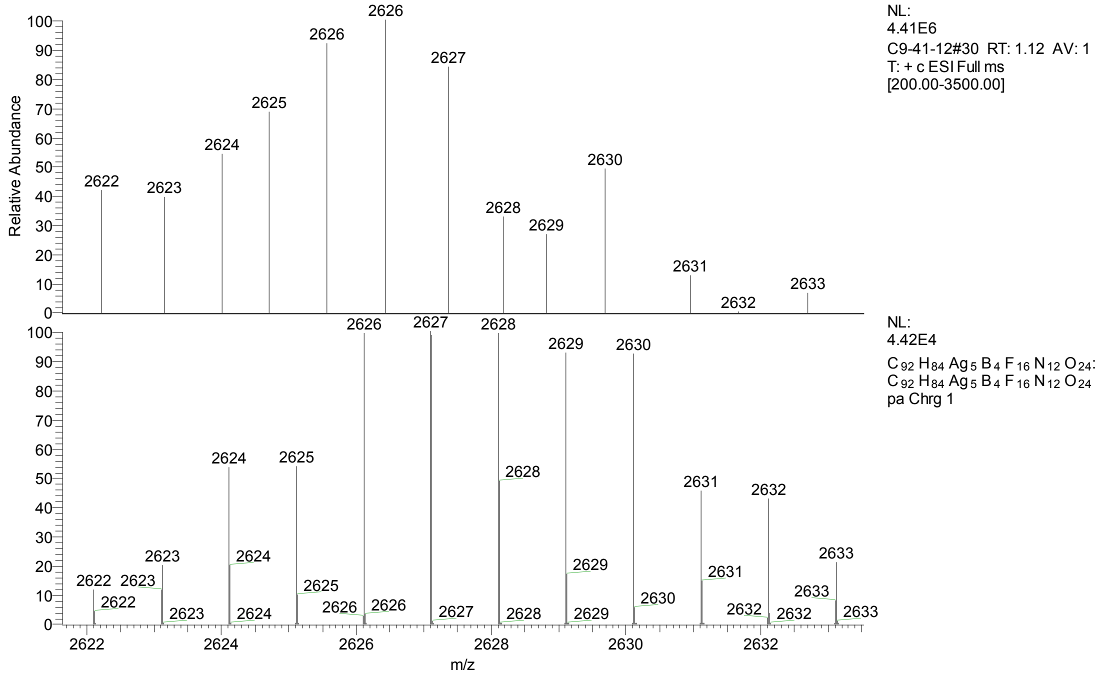

Figure 7. Calculated (down) and experimental (up) ESI-MS mass spectra of $Ag_5L_4(BF_4)_4^+$.

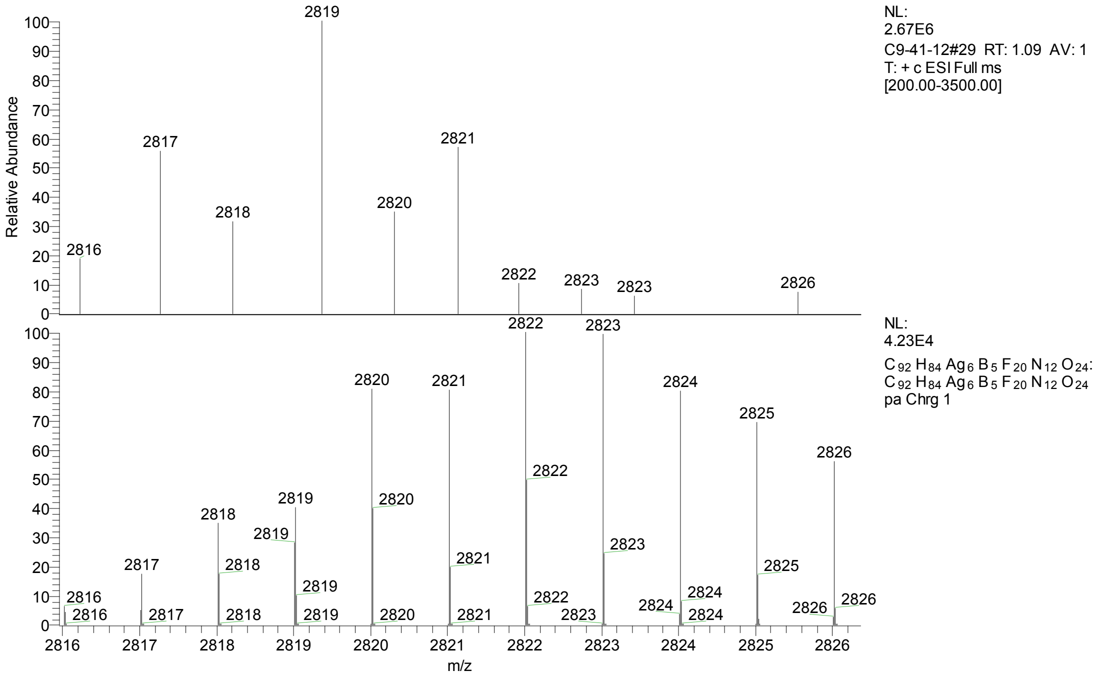

Figure 8. Calculated (down) and experimental (up) ESI-MS mass spectra of $Ag_6L_4(BF_4)_5^+$.

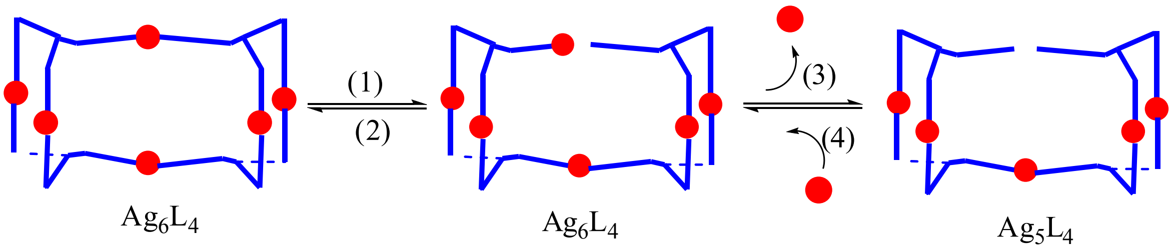

Scheme 2. The ESI-MS demonstrate that a dynamic equilibrium based on Ag_6L_4 cage in the solution of compound **1**.

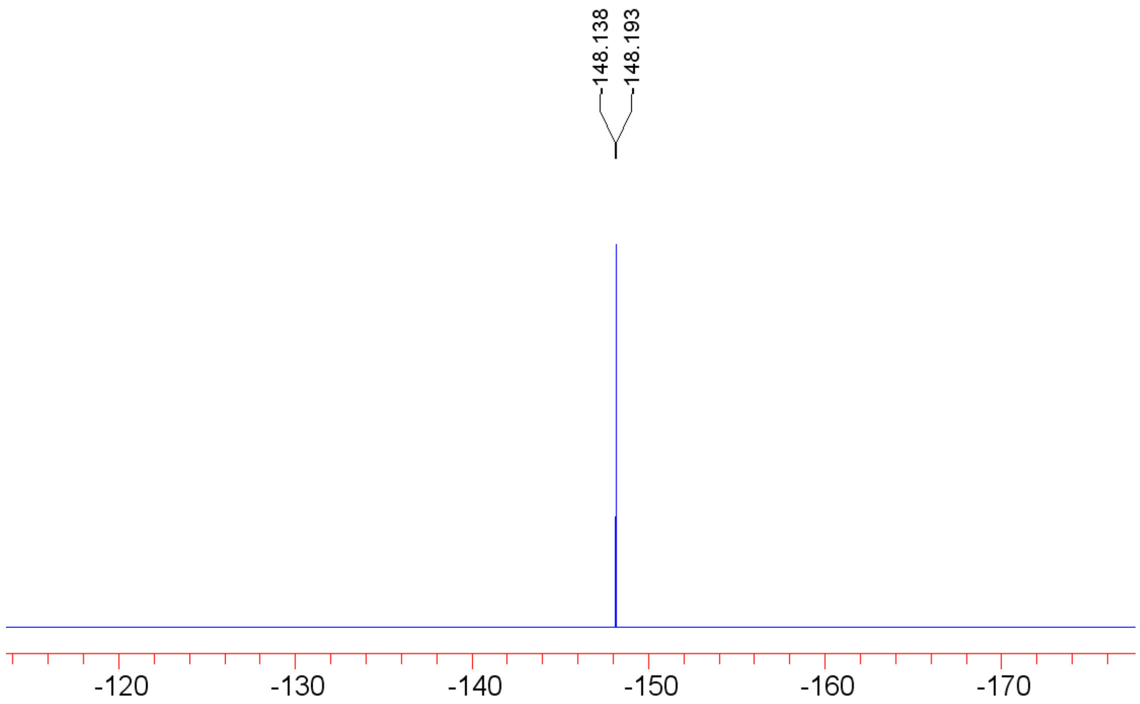

Figure 9. ^{19}FNMR (400 MHz, DMSO) of pure $AgBF_4$.

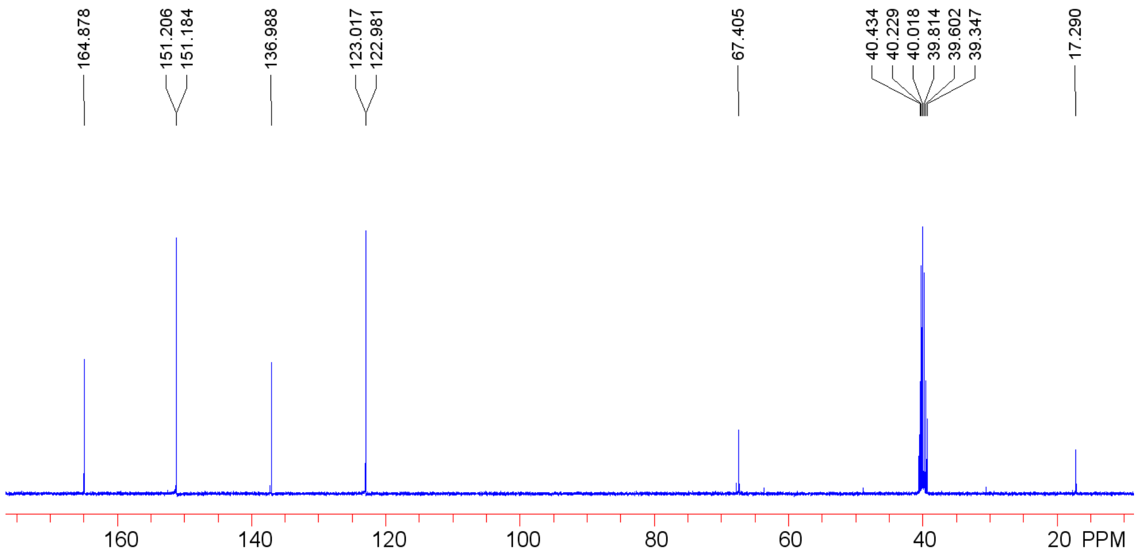

Figure 10. ^{13}CNMR (400 MHz, DMSO) of ligand **L** (**L**=tris(isonicotinoxymethyl)ethane).

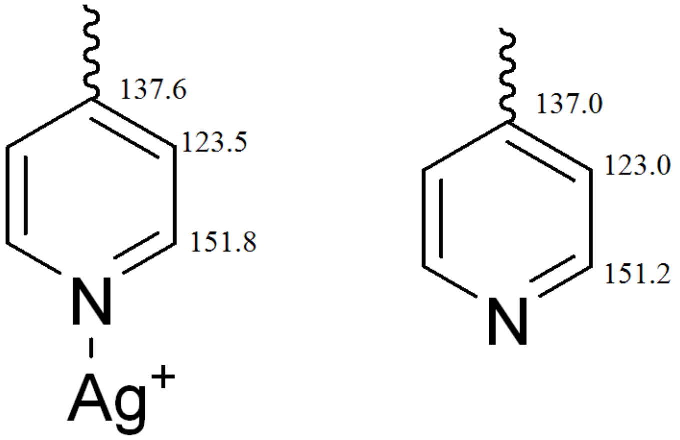

Scheme 3. Figure 2 and Figure 7 demonstrate that the differences between free ligand **L** and Ag coordinated ligand **L**, after coordinated with Ag, the ^{13}C-NMR spectra of pyridine ring all shift to down-field.

The ESI-MS spectrum of compound **1** (Figure 6) shows that there should contain Ag_6L_4 and Ag_5L_4 units, and may contain larger species, such as $(Ag_6L_4)_n$ and $(Ag_5L_4)_n$ units (n=2, 3…). However, the EA and solid ^{13}CNMR of compound **1** (Figure 5) demonstrate that the solid state of compound **1** should be Ag_6L_4 or $(Ag_6L_4)_n$ units; and the ^{19}FNMR (Figure 3, 9, 22-24) and solid ^{19}FNMR spectra (Figure 4, 12) demonstrate that there should have not interlocking products $(Ag_6L_4)_n$ such as [2]catenane, polycatenane in the solid state of compound **1**((Figures 12,22-24) show that the F atoms linked to two Ag atoms in the interlocking knots are shifted to down-field). So the compound **1** (solid state) is a discrete cage Ag_6L_4, while the Ag_5L_4 unit we observed in the ESI-MS is only available in the solution of compound **1** (Scheme 2) rather than in the solid state of compound **1**.

Synthesis of compound 2

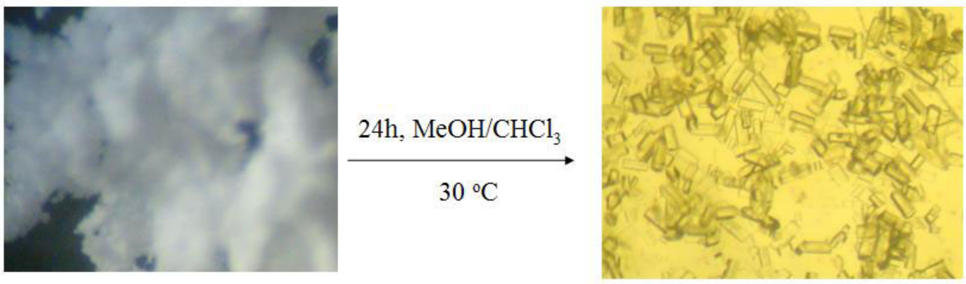

Figure 11. The *in situ* transformation of compound **1** (white solid) into compound **2** (transparent crystal) in the 2mL (MeOH/CHCl$_3$= 1/1) solution.

Continue soaking the 10 mg compound **1** in the 30°C 2 mL (MeOH/CHCl$_3$=1/1) solution within 24h gave a colorless rectangular crystal compound **2** (9mg, 90%). Anal. Calcd for [Ag$_6$L$_4$(BF$_4$)$_6$.1.3CHCl$_3$]$_n$ (%): C, 36.56; H, 2.81; N, 5.48; Found (%): C, 36.24; H, 3.23; N, 5.64. IR (KBr) *v* : 3437, 2973, 1733, 1563, 1409, 1287, 1122, 1083, 1063, 852, 757, 706, 681, 522 cm^{-1}. Solid ^{19}FNMR δ: -152, -133.

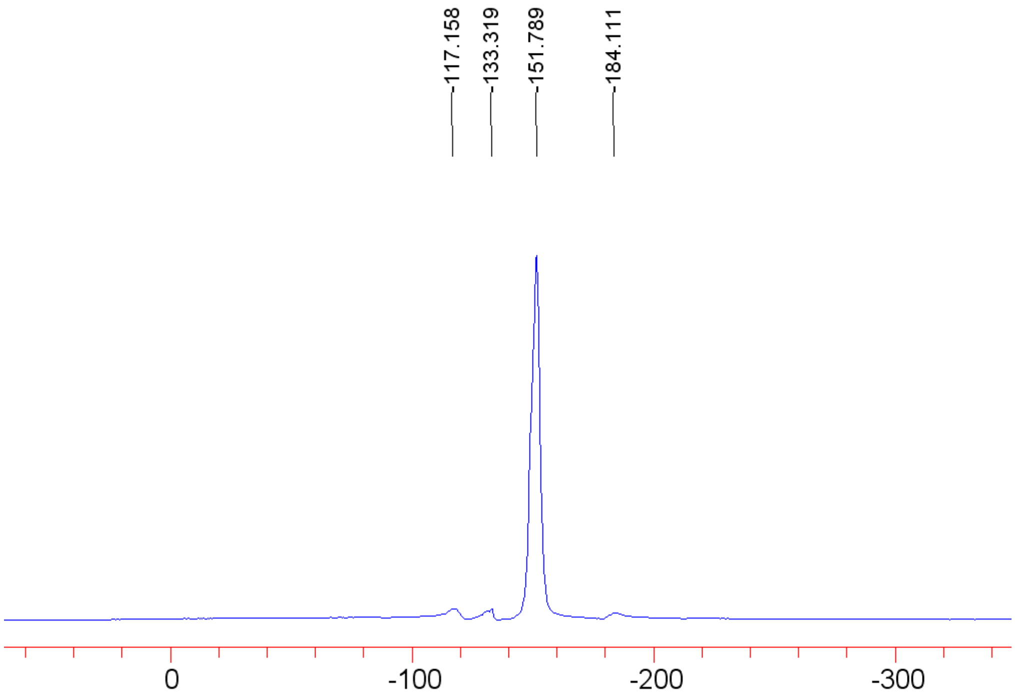

Figure 12. Solid ^{19}FNMR(500M) of compound **2**, in which the signals (-117 and -184) responds to the spinning sidebands of signal of -152.

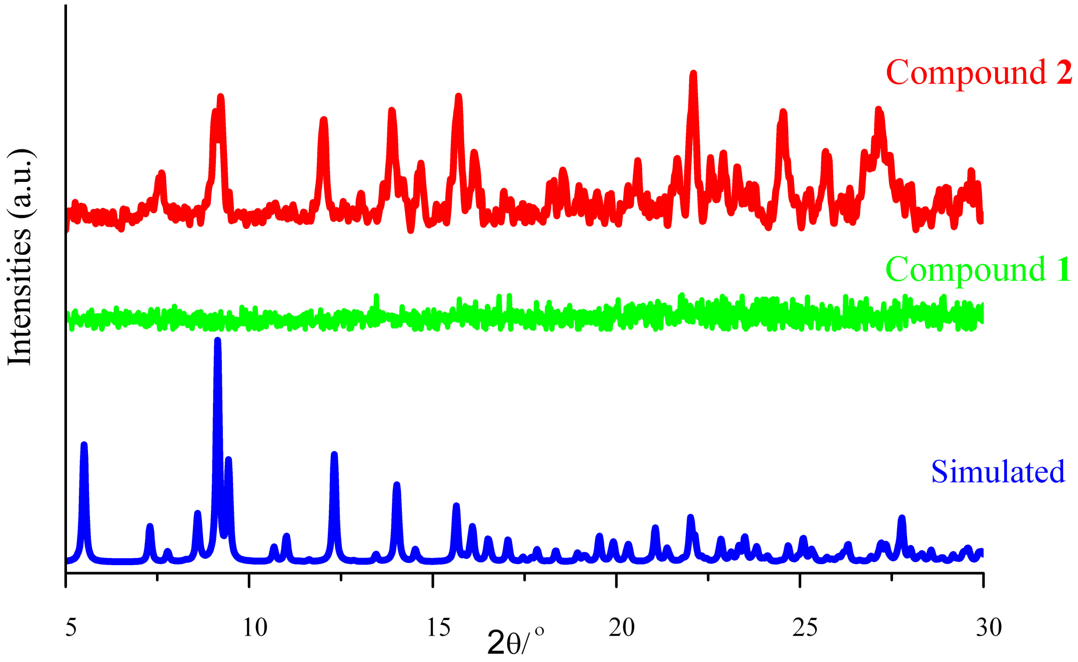

Figure 13. The powder x-ray diffraction spectra: from compound **1** to compound **2**.

Synthesis of compound 3

Method I: Dissolving 10 mg compound **1** in 15 mL (MeOH/$CHCl_3$=1/1), removing the insoluble compound **1** by filtering, adding another 5 mL (MeOH/$CHCl_3$=1/1) into the filtrate, sealed the 20 mL unsaturated solution of compound **1** at room temperature 30 days gave a colorless rhombic crystal, compound **3** (< 1 mg).

Method II: Continue soaking the 3 mg compound **2** in the 30°C 4 mL (MeOH/$CHCl_3$=1/1) solution 30 days gave a colorless rhombic crystal, compound **3** (1mg, 33%). Anal. Calcd for $[Ag_6L_4(BF_4)_6.MeOH.CHCl_3]_n$ (%): C, 36.88; H, 2.93; N, 5.49; Found (%): C, 36.89; H, 3.36; N, 5.57. IR (KBr) ν : 3452, 3107, 1733, 1614, 1424, 1282, 1123, 1063, 760, 702, 662, 476 cm^{-1}.

X-ray crystallography

Data collections were all performed on a Mercury CCD diffractometer with graphite monochromated Mo Ka radiation (λ = 0.71073 Å). The structures were solved by direct methods, and all calculations were performed using the SHELXL package[1]. The structures 2 - 3 were refined by full matrix least-squares with anisotropic displacement parameters for non-hydrogen atoms. All hydrogen atoms were generated geometrically and treated as riding. We employed PLATON/SQUEEZE[2-3] to calculate the contribution to the diffraction from the solvent region and thereby produced a set of solvent-free diffraction intensities. The final formula was calculated from the SQUEEZE[2-3] results combined with elemental analysis data. The crystallographic data are summarized in Table 1 and Table 2. CCDC 932526, 932527 contain the supplementary crystallographic data for 2, 3. These data can be obtained free of charge from The Cambridge Crystallographic Data Centre via www.ccdc.cam.ac.uk/data_request/cif.

Table 1. Crystal data and structure determination summary for **2**–**3**.

	2	**3**
CCDC deposit no.	932526	932527
Formula[a-b]	$C_{93.30}H_{85.30}Ag_6B_6Cl_{3.90}F_{24}N_{12}O_{24}$	$C_{47}H_{44.50}Ag_3B_3Cl_{1.50}F_{12}N_6O_{12.50}$
Formula weight	3064.97	1530.60
Crystal system	Tetragonal	Monoclinic
Space group	$P\text{-}42_1c$	$C2/m$
a (Å)	22.7000(18)	16.213(4)
b (Å)	22.7000(18)	23.949(5)
c (Å)	24.198(3)	18.894(4)
α (°)	90	90
β (°)	90	105.065(4)
γ (°)	90	90
V (Å^3)	12469.1(19)	7084(3)
Z	4	4
D_c (g/cm^{-3})	1.633	1.435
μ (mm^{-1})	1.111	0.961
F(0 0 0)	6062	3032
Crystal size (mm^3)	0.20x0.20x0.20	0.20x0.20x0.20
θ range (°)	2.01, 27.46	2.43, 27.48
No. of unique reflections / collected	14131/96947	8241/27871

Goodness-of-fit (GOF)	1.066	1.013
Final *R* indices ($I > 2\sigma(I)$)	0.0697	0.1028
R indices (all data)	0.0714	0.1195

a) The composition of solvent in compound **2** is determined by Elemental analysis;

b) The Elemental analysis of compound **3** shows that it contains $CHCl_3$ and MeOH molecules, and BF_4^- anions; the exact composition is hard to determine because the solvent is easy removed from compound **3** with large channels. Due to the large channel of compound **3**, the BF_4^- anions are disordered.

Table 2. Selected bond lengths [Å] and angles [°] for **2-3**

2			
Ag(1)—N(6)	2.176 (6)	Ag(3)—N(3)	2.141 (6)
Ag(1)—N(6A)	2.176 (6)	Ag(3)—N(5)	2.164 (6)
Ag(2)—N(2)	2.101 (6)	Ag(4)—N(1)	2.135 (7)
Ag(2)—N(4)	2.105 (6)	Ag(4)—N(1A)	2.135 (7)
N(6)—Ag(1)—N(6A)	176.1 (4)	N(3)—Ag(3)—N(5)	175.0 (2)
N(2)—Ag(2)—N(4)	166.4 (3)	N(1)—Ag(4)—N(1A)	177.1 (4)
Symmetry codes: (A) *-x*, *1-y*, *z*.			
3			
Ag(1)—N(1)	2.123 (6)	Ag(2)—N(2A)	2.161 (6)
Ag(1)—N(1A)	2.123 (6)	Ag(3)—N(3)	2.136 (7)
Ag(2)—N(2)	2.161 (6)	Ag(3—N3B)	2.136 (7)
Ag(3)—Ag(3C)	2.977 (3)		
N(2)—Ag(2)—N(2A)	174.3 (3)	N(1)—Ag(1)—N(1A)	177.9 (3)
N(3)—Ag(3)—N(3B)	165.5 (5)	N(3B)—Ag(3)—Ag(3C)	97.3 (2)
N(3)—Ag(3)—Ag(3C)	97.3 (2)		
Symmetry codes: (A) *x*, *-y*, *z*; (B) *-x*, *y*, *-z* ; (C) *-x*, *-1-y*, *-z*.			

Partial structures of compounds **2** and **3** are summarized in Figures 14-21:

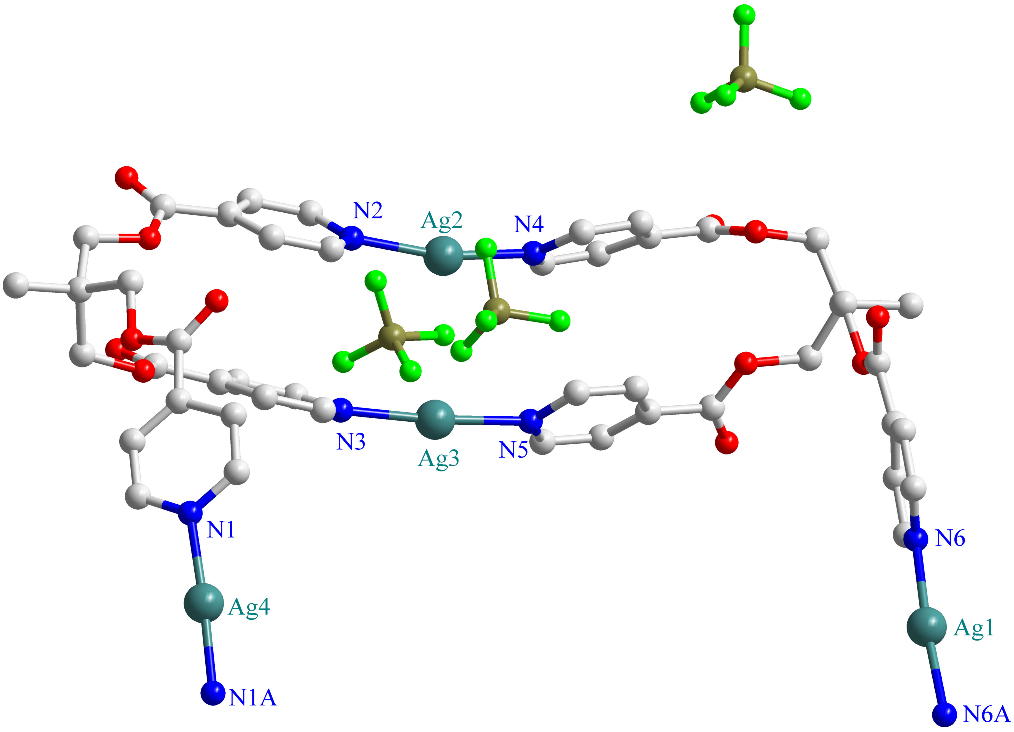

Figure 14. Coordination environment of compound **2**, for clarity, the hydrogen atoms are omitted.

Symmetry code: (A) -*x*, *1-y*, *z*.

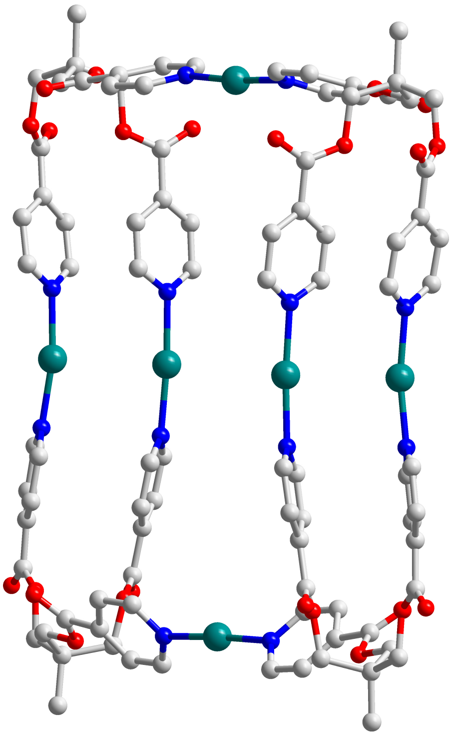

Figure 15. The Ag_6L_4 cage unit in Compound **2** (H atoms have been omitted for clarity).

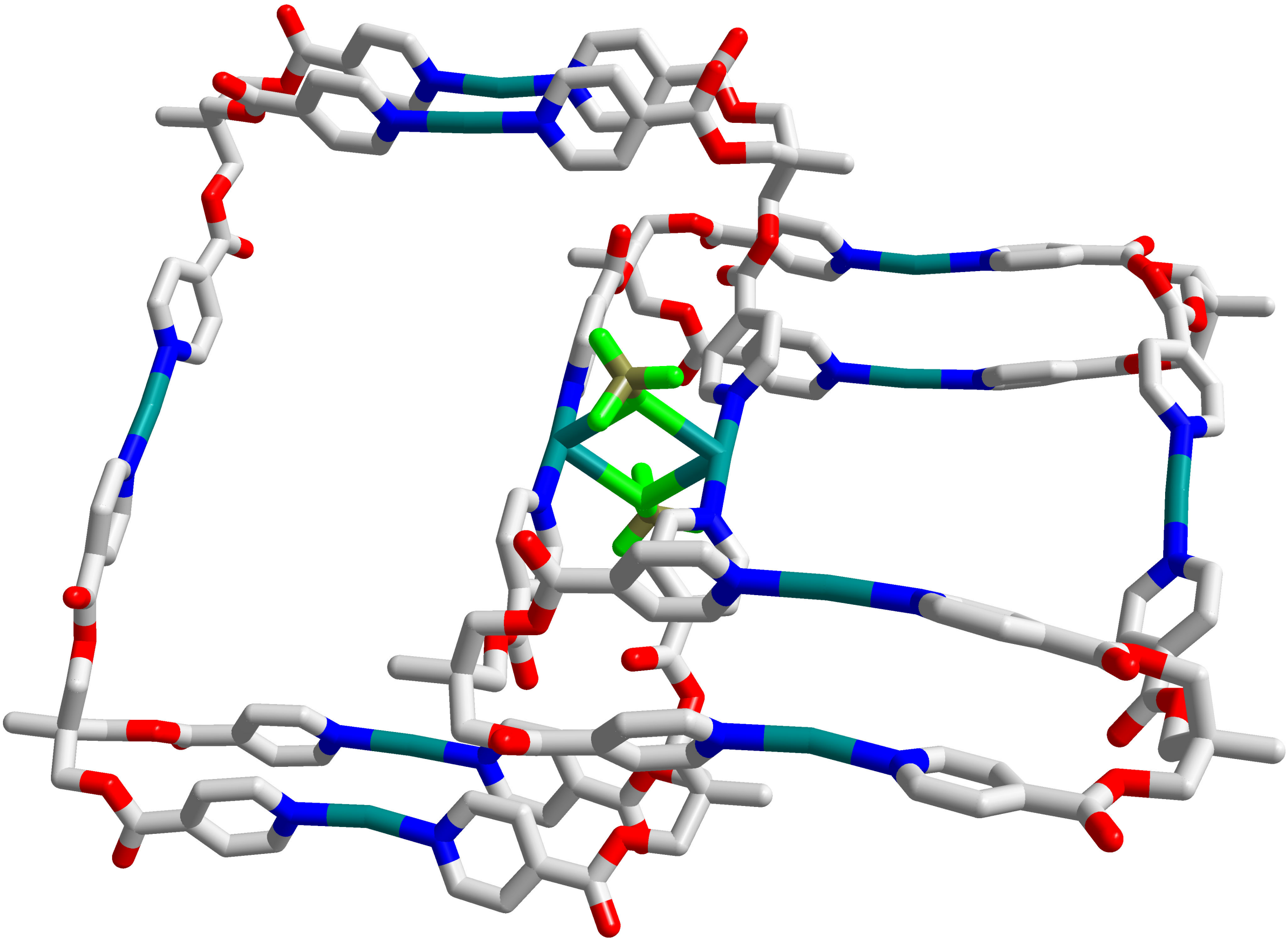

Figure 16. The charge-charge interaction between BF_4^- and Ag(I), which stabilizes the interlocking.

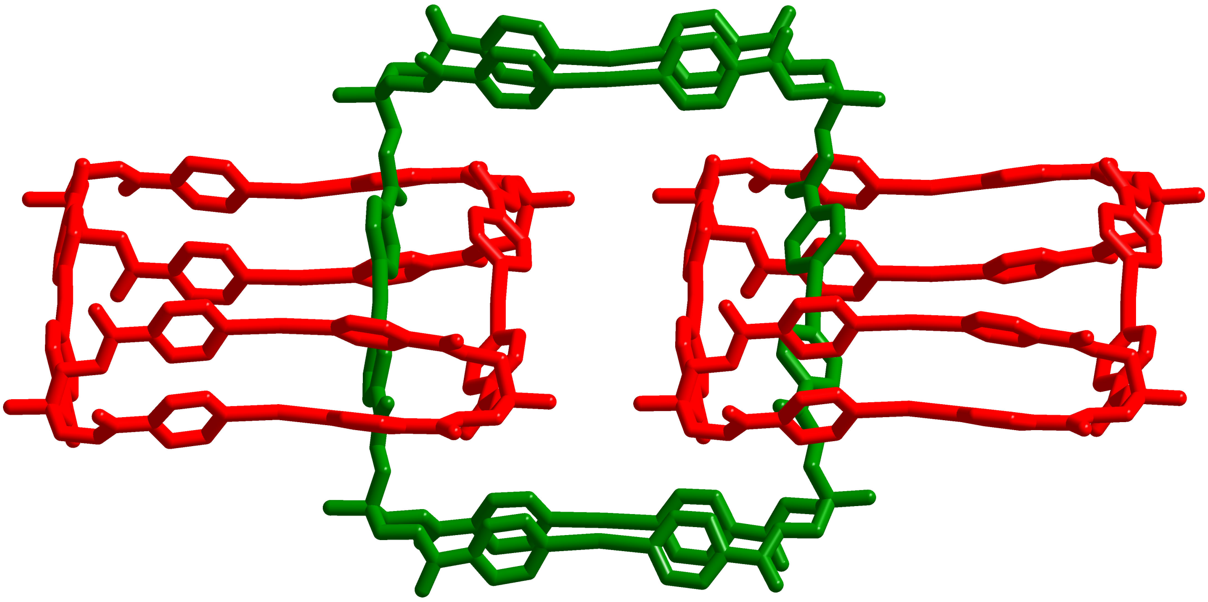

Figure 17. Structural fragment containing three interlaced metallacages in compound **2**.

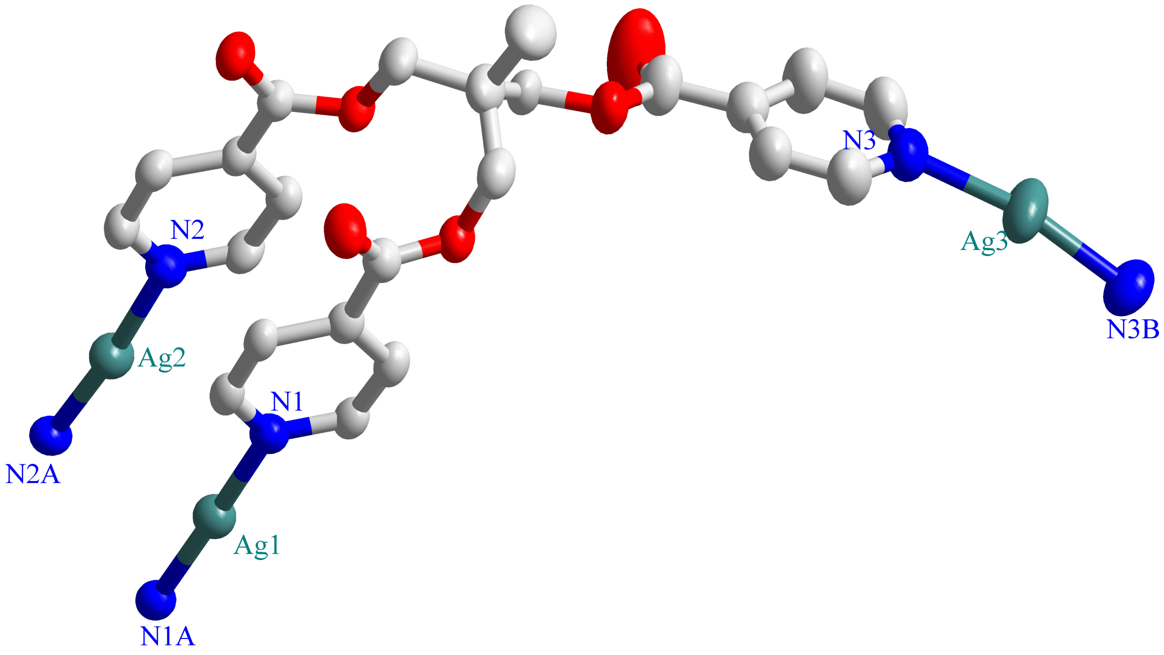

Figure 18. Coordination environment of compound **3**, for clarity, the hydrogen atoms are omitted. Symmetry code: (A) *x*, -*y*, *z*; (B) -*x*, *y*, -*z*.

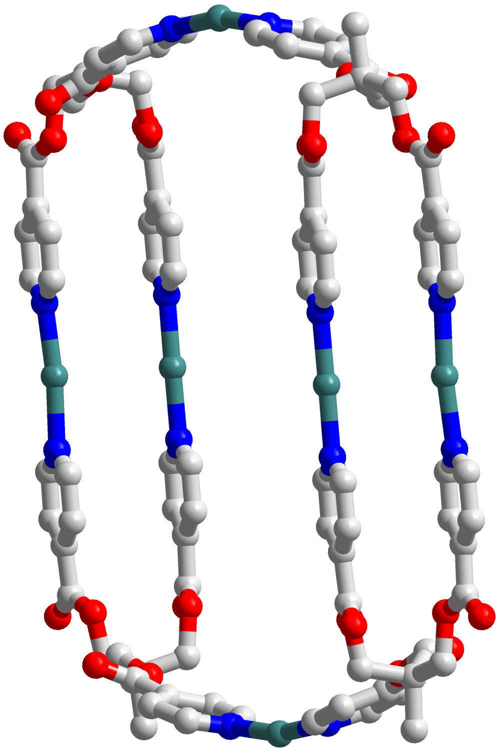

Figure 19. The Ag_6L_4 cage in **3**. (H atoms have been omitted for clarity).

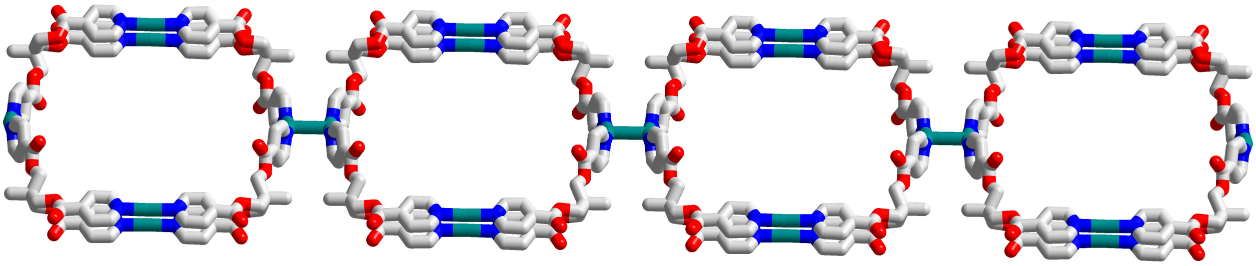

Figure 20. The Ag_6L_4 cages link directly into polycage chain.

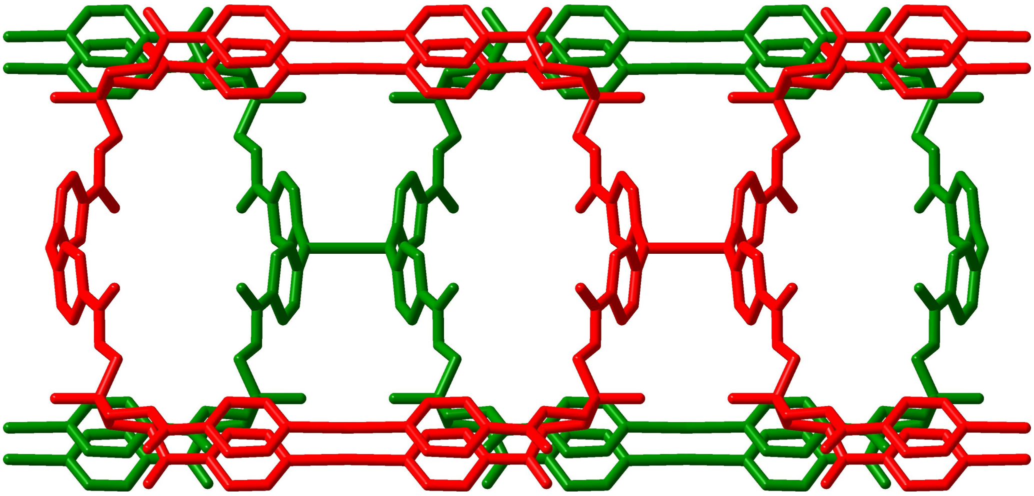

Figure 21. The polycage chain are stacked by AB style along the *a* axis, so the BF_4^- are disordered in their cavity.

Degradation of polycatenane into discrete cage.

Scheme 4. DMSO improved degradation of polycatenane into discrete cage.

Dissolving the 20mg compound **2** in the 1 mL DMSO-d6 solution, the process was recorded by ^{19}F-NMR, Figure 19 shows that there are many interlocking knots in the solution, Figure 20 demonstrates that the interlocking knots are reduced 1 day later,

Figure 21 demonstrates that nearly no interlocking knots are available in the solution after 2 days. The ^{13}C-NMR and ESI demonstrate that the Ag_6L_4 cages are available and stable in the DMSO solution (Figure 22- Figure 23).

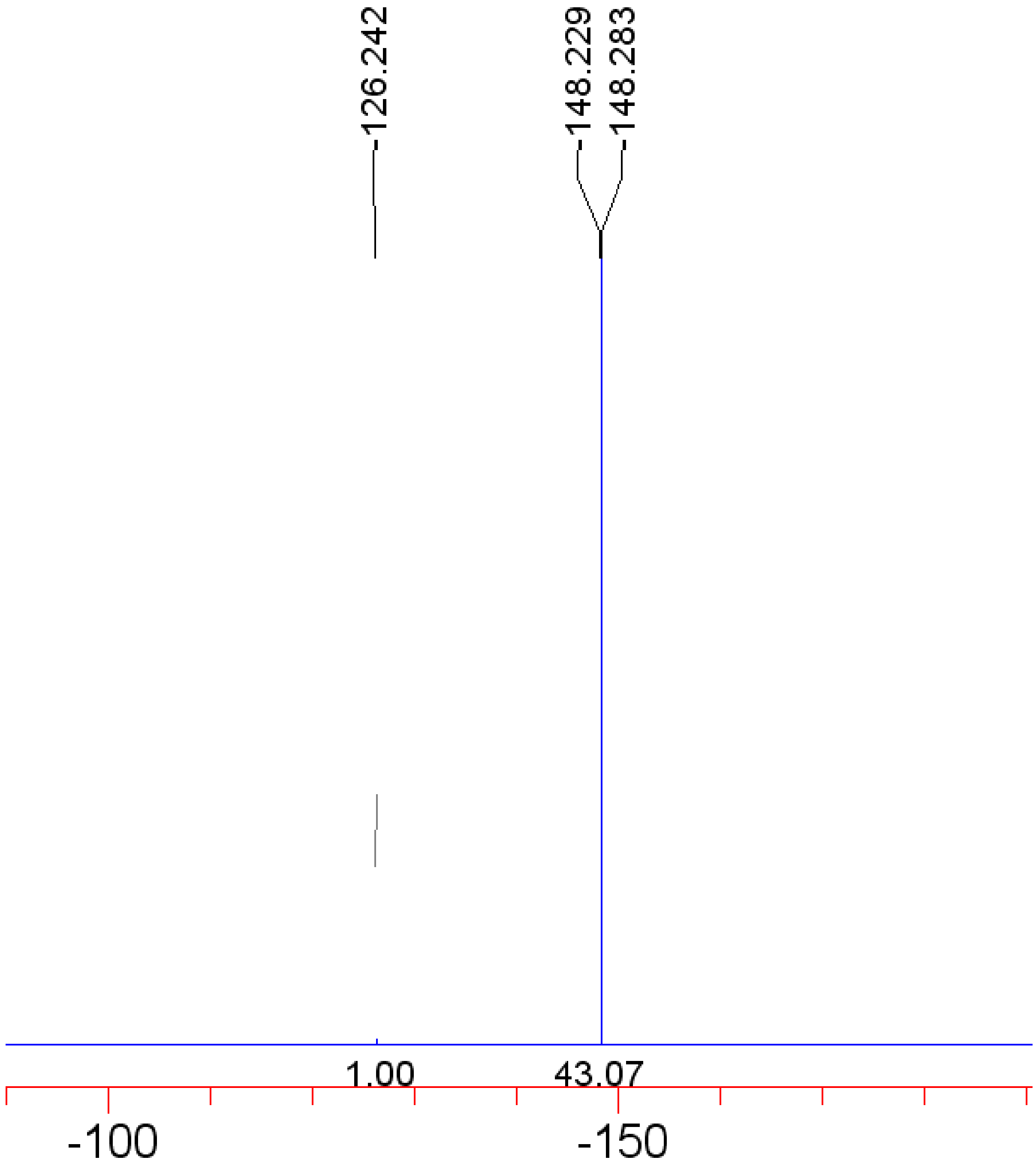

Figure 22. The *in situ* ^{19}F-NMRof DMSO solution of compound **2**.

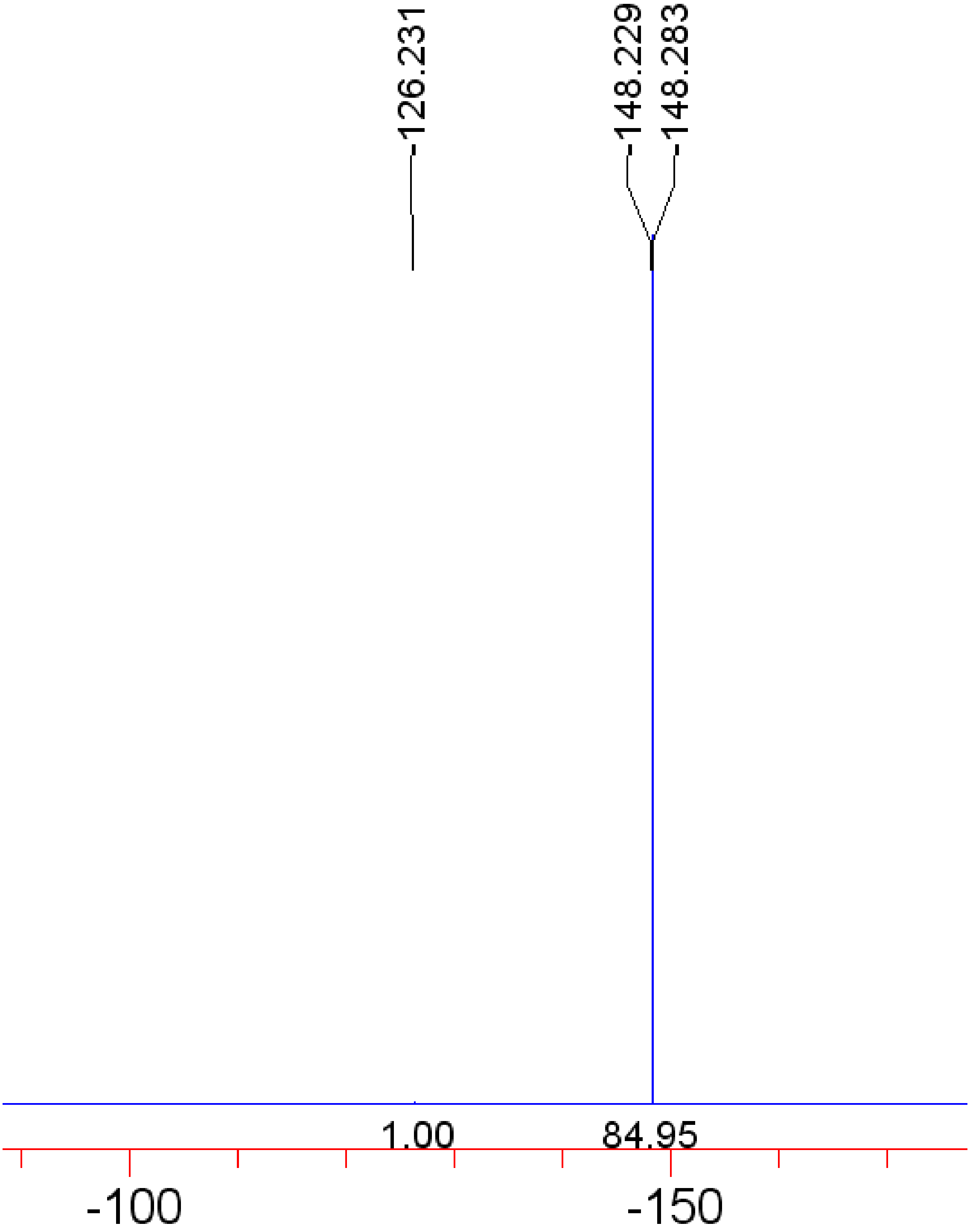

Figure 23. The ^{19}F-NMRof DMSO solution of compound **2** (one day later).

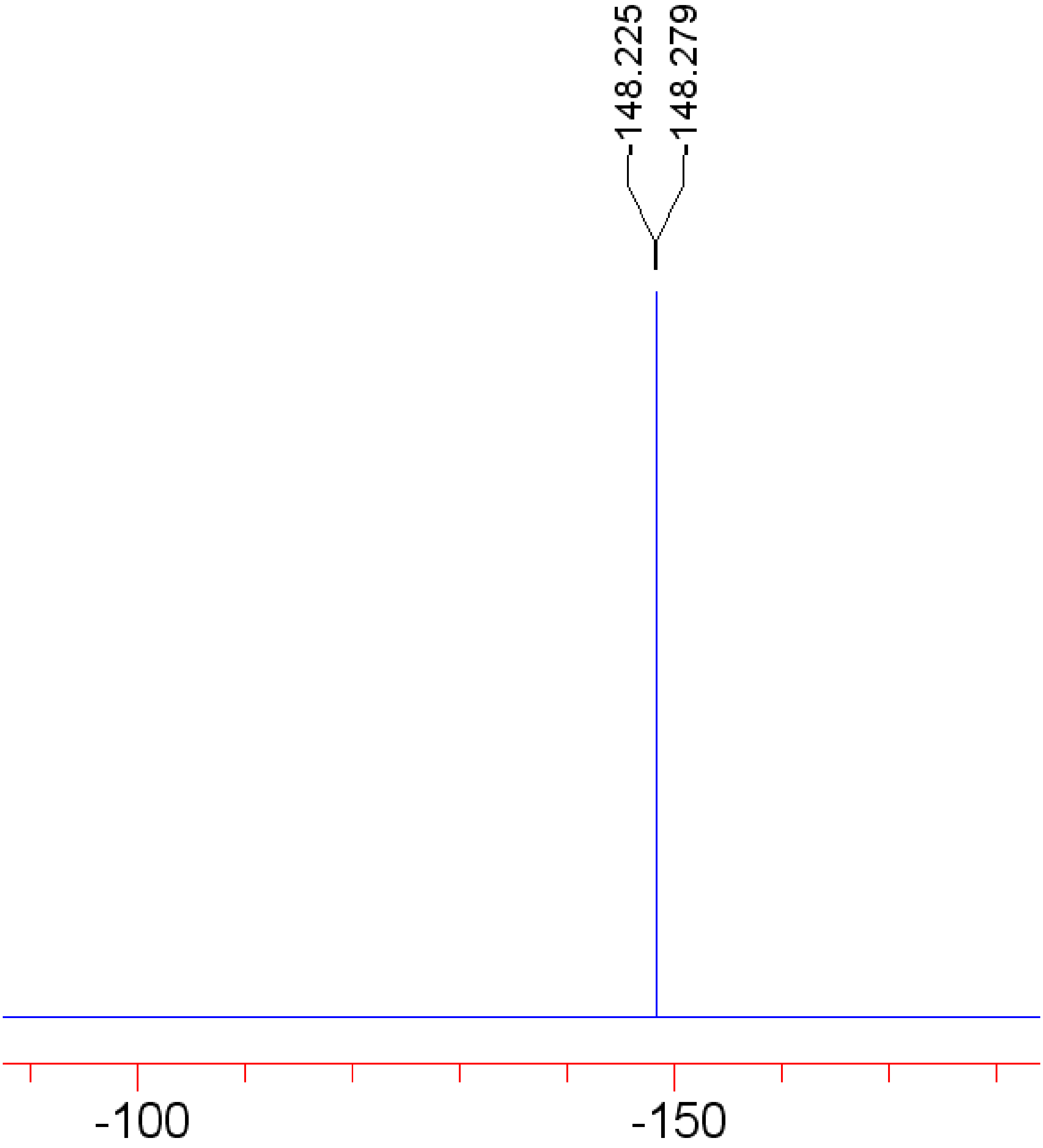

Figure 24. The ^{19}F-NMRof DMSO solution of compound **2** (two days later).

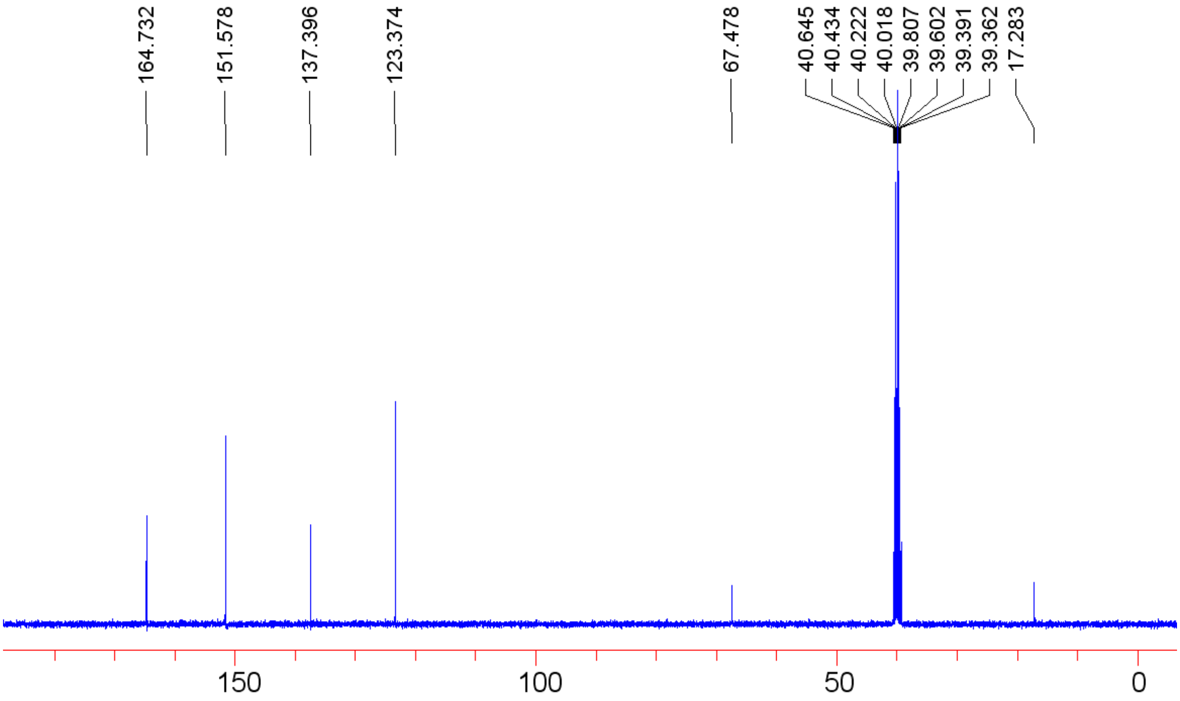

Figure 25. The^{13}C-NMRof DMSO solution of compound **2** (two days later).

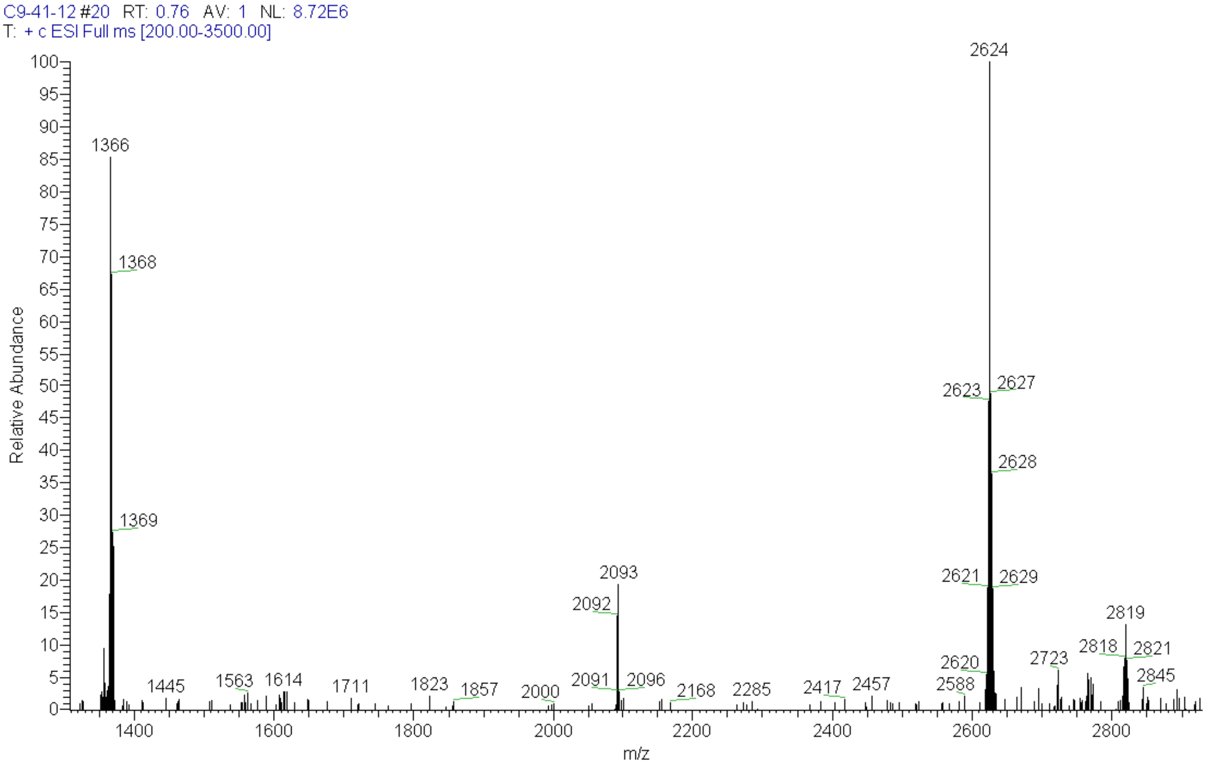

Figure 26. The ESI-MS of DMSO solution of compound **2** (two days later).

1. G. M. Sheldrick, *SHELXTL-97,* Program for the Solution of Crystal Structures*,* University of Göttingen, Germany, 1997.
2. A. L. Spek, Single-crystal structure validation with the program *PLATON. J. Appl. Crystallogr.*, 2003, **36**, 7-13.
3. P. Van Der Sluis, A. L. Spek, BYPASS: an effective method for the refinement of crystal structures containing disordered solvent regions. *Acta Crystallogr., Sect. A*, 1990, **46**, 194-201.